**IMPROVEMENT OF VALLEY NETWORK 3D GEOMETRY FROM HRSC DEMS COMPARED TO MOLA DATA.**

V. Ansan[1] , N. Mangold[1], Ph. Masson[1], G. Neukum[2] and the HRSC co-Investigator team. [1] Lab. IDES-CNRS UMR8148, bât. 509, CNRS and Université Paris-Sud, 91405 ORSAY, France, [2] DLR, Berlin, Germany, Contact: veronique.ansan@u-psud.fr, nicolas.mangold@u-psud.fr

**Introduction:** Since visible images have been acquired by Viking orbiter in 1976, valley networks have been mainly identified in the heavily cratered uplands dated Noachian (>3.5 Gyr). Valley networks on Mars have been the subject of considerable debates about their formation processes since three decades [1-5].

At the end of 1990's, the Mars Orbiter LASER Altimeter (MOLA) provided a new vision of the Mars topography with a great vertical accuracy of ~50 cm [6]. These altimetric data gave the possibility to study the geometry and topography of valley networks at spatial resolution of typically 500m -1 km [e.g. 7]. This resolution is sufficient to map large valleys but not small tributaries that we can map on high resolution imagery.

Since 2004, the Mars Express High Resolution Stereo Camera (HRSC) on board of Mars Express orbiter has acquired visual images in stereoscopic mode [8] with typical spatial resolution of ~10m for the nadir images. From nadir and stereoscopic images, Digital Elevation Models (DEM) can be generated with a typical spatial resolution of ~50 m or lesser depending on that of input images, but the vertical resolution is not as good as that of MOLA, typically 20 to 100 m depending on terrains roughness and image quality [8-10].

In this study, we compare the organization of valley networks in three regions (region near Huygens impact crater, Aeolis region and West Echus Chasma plateau) using both DEMs (MOLA and HRSC) and manual mapping in order to quantify the difference of geometry between these datasets.

**Generation of HRSC DEMs:** HRSC camera acquired images in five panchromatic channels under different observation angles and four colour channels at relatively high spatial resolution [8]. In our work, we used only three panchromatic channels acquired at the nadir in which the spatial resolution reaches generally ~10 m/pixel, and the two stereoscopic images with a spatial resolution twice to three times lesser.

We use the photogrammetric software developed both at the DLR and the Technical University of Berlin [9-11], in order to generate HRSC DEMs. Here, we summarise the different steps for obtaining them. The first step corresponds to the rectification of nadir and stereo images at the same scale. We often apply them a median filter to remove or decrease the noise in the rectified images.

The second step consists of the image correlation to find the location of homologous points in the different HRSC images, using a matching process at different spatial grid [9,11].

The third step corresponds to the calculation of the spatial location of 3D object points, defined by cartesian coordinates in a body-fixed Martian reference system, using the intersection of distances between the camera position and the location of homologous points in each HRSC image (stereomodel).

The fourth step corresponds to the transformation of cartesian coordinates of 3D object points in geographic latitude, longitude and height projected on the MARS IAU ellipsoid [12]. In order to compare the MOLA and the HRSC altimetry, we used the Martian geoid, i.e. areoid as the topographic reference for heights [13].

The last step consists of the generation DEM using VICAR image processing system [14] in which the gap areas are filled by height interpolation.

The horizontal spatial accuracy of DEM is often twice to three times the original image resolution and the height accuracy depends both on the geometric parameters of HRSC camera, the geometric resolution of images, the terrain roughness and the image quality.

**Extraction of valley networks:** First, we mapped manually the valley networks from the nadir images at ~10m/pixel, taking into account the geological context.

Second, we used a hydrologic analysis (DNR hydromod) included in ARCVIEW GIS [15] in order to extract the valley network from DEMs. The DNR hydromod program consists of three steps of processing : 1) the original topography (DEM) is modified removing sinks to produce a continuous flow direction grid; 2) a flow direction grid is calculated from the centre of cell to the steepest down-slope direction of the eight neighbouring cells (D8 algorithm); 3) a flow accumulation grid is generated as the cumulative number of cells flowing into each down-slope cell. Cells that have high accumulation of flow may be used to identify stream channels or valleys.

As the detection of stream channel is depending on the flow accumulation, the comparison of the organisation of valley networks into the same drainage basin (e.g. number of tributaries, spatial distribution…) from two DEMs at different spatial scales is mainly controlled by the threshold on the cumulative number of cells flowing into each down-slope one. For this reason, we determine a minimum thershold for MOLA. Then, we apply this threshold multiplied by the scale ratio between MOLA and HRSC DEM for detecting the stream channels into HRSC DEM.

The location of probable stream channels on Mars detected by DNR hydromod routine from the two DEMs is then checked with HRSC nadir images. Valley networks that are not visible in HRSC images (e.g. in flat areas, in closed depressions with flat interiors, in small impact craters…) are deleted. Only the lengths of individual valley network segments and the remaining area containing valley networks are used to determine the average drainage densities.

**Valley networks in region near Huygens crater:** The HRSC camera acquired images at resolution of 50m/pixel during the H0532 orbit, on the eastern rim of Huguens impact crater (Fig. 1) located at the north-western part of Hellas basin (the Iapygia quadrangle of Mars). This area is mainly old, hilly and cratered upland terrain[16], dated of Noachian [17] associated with intraplains dated of Hesperian [17].

The 475-km-diameter impact crater Huygens is the most important geological feature of this area. Its eastern boundary is characterized by numerous valley networks showing with a mature organisation (dendritic pattern with high bifurcation ratio) similar to that of terrestrial valley network in temperate climatic zones. These valley networks have large drainage basins and a high density drainage.

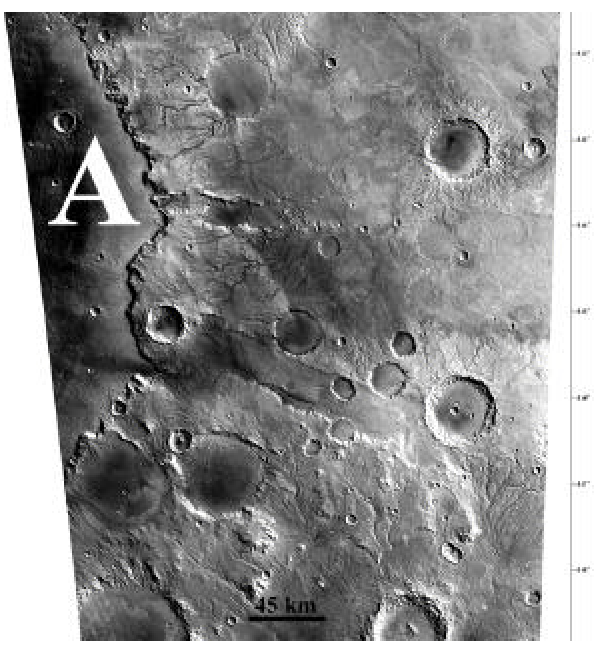


Figure 1. Extract of HRSC nadir image (H0532 orbit) at 50 m/pixel showing numerous valley networks on the eastern riù of Huygens impact crater (A).

The DEMs generated from stereo images give quantitative information about the morphometry of valleys. Using the triplet of images (nadir and two stereos ones), we generated by DLR's software [9] a DEM with a spatial resolution of 150m/pixel and a height accuracy of 24 m, which highly improves the topography of this area previously observed by MOLA data. However, the spatial resolution is not really good in comparison with MOLA data because of the bad spatial resolution of stereo images i.e. 71 m and 100 m respectively.

Despite the low resolution of HRSC DEM, one Strahler order greater than that detected from MOLA data is reached with a drainage density twice greater (0.1 and 0.3 $km^{-1}$). With manual mapping from nadir HRSC images at 50m/pixel, the drainage density can reach 0.5 $km^{-1}$ with 5 Strahler orders (Fig. 1).

**Valley networks in Aeolis region:** This region is characterized by densely cratered terrains dated of the Noachian period [18,19]. The terrains between large craters are incised by valley networks. HRSC acquired some nadir images with a spatial resolution ranging from 10 m to 40 m in Aeolis region.

These images show that the densely cratered terrain has been modified by numerous valley networks. The nadir images of 228 and 241 orbits, centered at 157.355°E and 30.576°S (Fig. 2) displays a set of valley networks with a mature organisation (dendritic pattern with high bifurcation ratio) similar to that of terrestrial valley network in temperate climatic zones.

A DEM has been generated with a spatial resolution of 30m/pixel and a height accuracy of 13 m, which highly improves the topography of this area previously observed by MOLA data.

We mapped automatically and manually the valley networks in the three datasets and the morphometric analysis gives us a new insights for these valley networks. MOLA drainage density gives between 0.1 and 0.2 $km^{-1}$ with Strahler order of 3 whereas HRSC DTM gives between 0.1 and 0.3 $km^{-1}$ with Strahler's order of 4. With manual mapping from nadir HRSC images at 22.4m/pixel, the drainage density is between 0.1 and 0.5 $km^{-1}$ with Strahler order of 5 (Fig. 2). HRSC DEM gives thus a strong improvement in the drainage characterization compared to MOLA, but still not sufficient to reproduce manual mapping.

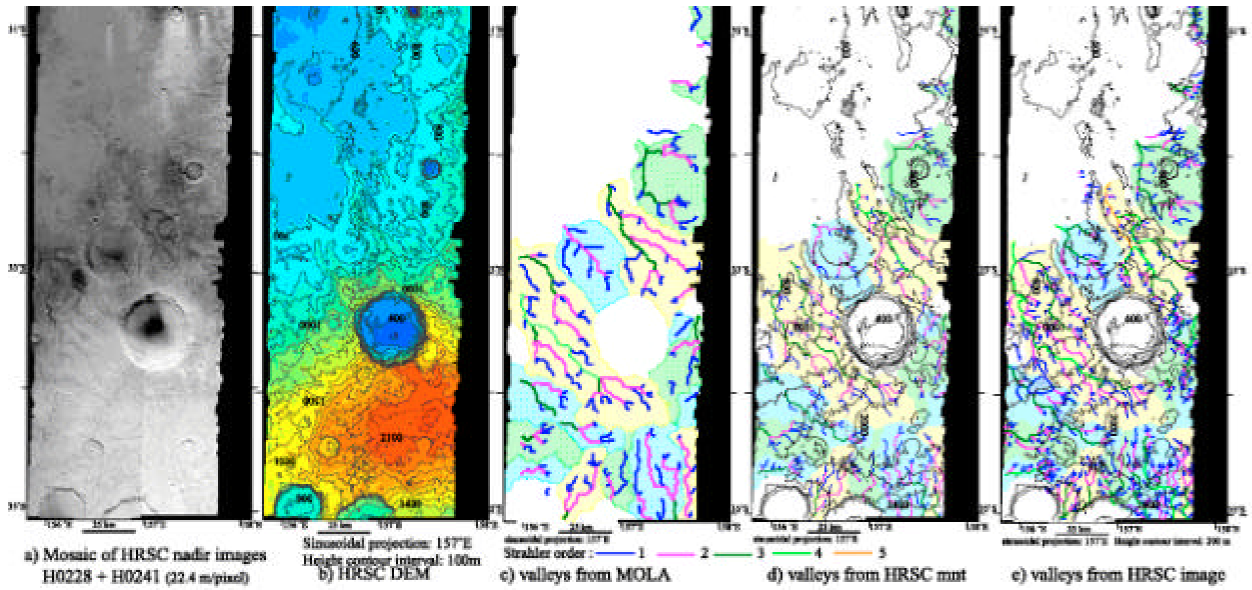


Figure 2. a) Extract of HRSC image (orbit H0228) located in Aeolis region. Numerous dendritic valley networks incised Noachian densely cratered terrains. b) HRSC DEM at resolution of 30m/pixel. Valley networks extracted from c) MOLA, d) HRSC DEM and e) HRSC images.

**Valley networks in Echus region:** This region is located on the plateau at the west of Echus Chasma canyon (278-281°E, 0-5°N). Valley networks were identified the first time from their difference of thermal properties on THEMIS images [20].

HRSC images provide the possibility to analyse in details their morphology and geometry with the spatial resolution at ~20 m/pixel (Fig. 3). Valleys in Echus area are not restricted to the locations where they have been observed through THEMIS images [20]. They extend over more than 200 km along Echus Chasma western plateau. A HRSC DEM has been generated with a spatial resolution of 50m.

Once again, a manual and automatic detection of valley networks have been performed respectively from HRSC image, HRSC DEM and MOLA DEM. For example, a drainage basin included in an old filled impact crater shows an organisation of 2 Strahler's order at MOLA scale, 3 orders for HRSC DTM and 4 for HRSC nadir image mapping. We thus detected 3 times more valleys with HRSC DEM than with MOLA data.

In the three examples, the detection of valley networks is significantly improved from HRSC DEM, but it is nevertheless far to be comparable with the manual mapping which is able to identify the smallest tributaries. With the manual mapping, these valley networks display a mature dendritic pattern with high bifurcation ratio [21,22] ranging from 3 to 5.

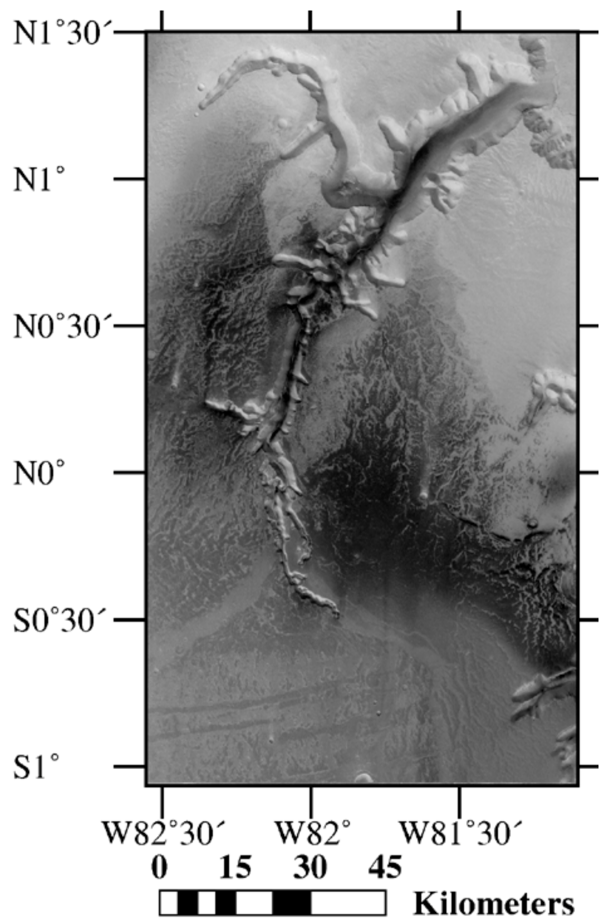


Figure 3. Extract of HRSC nadir image (H2204 orbit) at resolution of 20 m/pixel. See the dendritic pattern of valley networks on each side of Echus canyon.

**Valley geometry:** Differents studies have been made from MOLA data to estimate the width, depth and side slope of valleys on Mars [23,24]. MOLA topography enable us to detect only a few valleys in these three regions with depth of about 100 m (Fig.4, grey line). This is mainly due to the widths of valleys. Indeed, valleys less than 500 m wide can not be detected in MOLA DEM despite the excellent vertical resolution. In contrast, HRSC DEMs at spatial resolution of ~50m give slightly better results by detecting most valleys deeper than 30 m (Fig.4, black line).

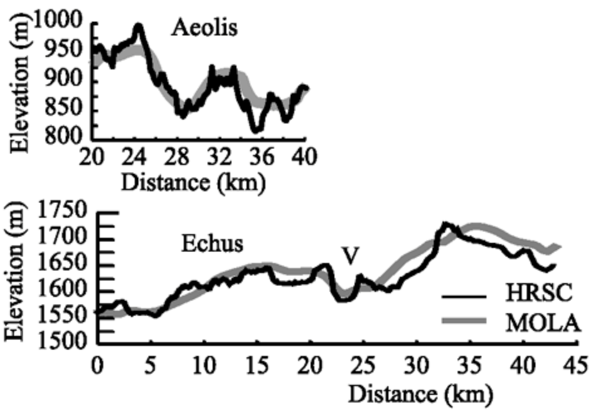


Figure 4. Transversal topographic profiles extracted from MOLA and HRSC DEMs in Aeolis and Echus regions.

**Conclusion:** Compared to MOLA, HRSC DEMs improve the quantification of valley networks properties such as drainage densities and aspect ratios, showing that the manual mapping of valleys with previous Viking or THEMIS images were justified.

Nevertheless, mapping from HRSC images show that the manual mapping is still better than any automatic method and will continue to be useful to characterize valleys, at least in 2D.

The three studied regions enable us to compare Noachian (Huygens and Aeolis regions) and Hesperian (Echus plateau) valley networks. The comparison shows that the West Echus plateau younger drainages are much more shallow with less incision than in Noachian regions, despite that the drainage densities is higher and their maturity is large. This difference is probably the effect of three parameters: (1) Noachian terrains are not as well preserved as late episodes of activity on freshly formed Hesperian rocks, possibly explaining small tributaries are missing over Noachian terrains, (2) the duration of Noachian networks might be longer to explain the larger incision of valleys, (3) the bedrock composition is uncertain and might be different. Such automatic studies will be continued over larger area to be statistically valid and improve our understanding of Martian valley networks.

**References:** [1] Carr, M. H. and Chuang, F. C. (1997) *JGR*, 102, 9145-9152. [2] Baker, V. R. and Partridge, R. C. (1986) *JGR*, 91, 3561-3572. [3] Gulick, V. C. (2001) *Geomorphology*, 37, 241-268. [4] Cabrol, N. A. and Grin, E. A. (2001) *Geomorphology*, 37, 269-287. [5] Pieri, D. C. (1980) *Science*, 210, 895-897. [6] Smith, D.E (1998) *Science 279*, 1686-1692. [7] Stepinski T.F. and Stepinski A. P (2005) *JGR*, 110, E12S12. [8] Neukum G. et al. (2004) *ESA Special Publication*, SP-1240. [9] Scholten et al. (2005) *Photogram. Eng. Rem. Sens.*,71, 1143-1152. [10] Jaumann et al. (2007) *Planetary & Space Science* 2172. [11] Albertz J. et al. (2005) *Photogram. Eng. Rem. Sens.*, 71 (10), 1153-1166. [12] Duxbury T. C et al. (2002) *Symposium on Geospatial Theory, Processing and Application*, Ottawa. [13] Smith, D. E (1999) *Science*, 286, 94-97. [14] MILP (2005) URL: http://www-milp.jpl.nasa.gov/ [15] Loesch, T. N. (2001). Spring Workshop. [16] G. Schaber (1977) Iapygia (MC-21) 1:5,000,000, map I-10-20. [17] Greeley R. & Guest J. J. (1987) USGS Maps I-1802-B. [18] Scott, D. H. et al. (1978) USGS map- I-1111 (MC-23). [19] Tanaka, K. L. (1986). *JGR 91*, E139-E158. [20] Mangold N. et al. (2004) Science 305, 78-81. [21] Horton, R. E. (1945) *Geol. Soc. Am Bull*.., 82, 1355-1376, 1945. [22] Leopold L. B. et al. (1992) *Fluvial processes in geomorphology*, 520 pp. [23] Williams, R. and Phillips R. J. (2001) *JGR* 106, 23737-23751. [24] Ansan V. and Mangold N. (2006) *Planetary and Space Science* 54., 219-242.